ARCTIC
VOL. 44, SUPP. 1 (1991) P. 153-163

Lake and River Ice Investigations in Northern Manitoba Using Airborne SAR Imagery

ROBERT LECONTE[1] and P. DAVID KLASSEN[2]

(Received 6 June 1990; accepted in revised form 17 June 1991)

ABSTRACT. Multichannel airborne SAR data were collected over northern Manitoba in April 1989 and January 1990. During the week of the SAR flights, several reconnaissance helicopter flights were undertaken, and ground calibration sites were visited to collect ice, snow, and water data. A total of six SAR image passes were flown in April 1989 and seven in January 1990, in order to collect a data set with numerous incidence angle, frequency, polarization, and look direction combinations. The data have been qualitatively assessed, with specific emphasis on C-band horizontally polarized imagery — the proposed SAR configuration for Radarsat. Results of the analysis have shown that airborne SAR can be used to identify various freshwater ice features, such as juxtaposition ice, refrozen slush, river ice runs, and lake ice. Open water leads were also successfully identified. A careful interpretation of the airborne SAR imagery in conjunction with the ground truth data has shown that the unusually bright returns characterizing the Burntwood River and the west portion of Split Lake were caused by a layer of refrozen slush that was generated during the initial formation of the ice cover. Although the results reported here focused exclusively on a qualitative analysis of C-HH data, preliminary analysis of the digital data suggests that changes in frequency and polarization produce measurable differences and can be used to develop classification algorithms for freshwater ice.

Key words: synthetic aperture radar, fresh water ice

RÉSUMÉ. En avril 1989 et janvier 1990, on a recueilli des données à l'aide d'un radar multicanal à antenne synthétique aéroporté, au-dessus du nord du Manitoba. Au cours de la semaine des vols du radar à antenne synthétique, on a effectué plusieurs vols de reconnaissance en hélicoptère, et visité plusieurs sites terrestres d'étalonnage pour collecter des données sur la glace, la neige et l'eau. On a effectué au total six prises d'images en vol avec le radar à antenne synthétique en avril 1989, et sept en janvier 1990, dans le but de recueillir un ensemble de données comportant de nombreuses combinaisons d'angle d'incidence, fréquence, polarisation et orientation. On a évalué les données de façon qualitative, en insistant particulièrement sur les images polarisées horizontalement dans la bande C, qui est la configuration suggérée du radar à antenne synthétique pour Radarsat. Les résultats de l'analyse ont montré que le radar à antenne synthétique aéroporté peut être utilisé pour l'identification de divers attributs de la glace d'eau douce, tels que la glace de juxtaposition, la bouillie de regel, les descentes de glace fluviale et la glace de lac. On a aussi identifié avec succès les chenaux d'eau libre. Une interprétation minutieuse des images prises au radar à antenne synthétique aéroporté, jointe à des données terrestres fiables, a révélé que les échos brillants inhabituels qui caractérisent la rivière Burntwood et la partie ouest du lac Split, étaient dus à une couche de bouillie de regel datant du stade initial de formation de la couverture de glace. Bien que les résultats rapportés ici concernent exclusivement l'analyse qualitative des données polarisées HH dans la bande C, une analyse préliminaire des données numériques suggère que des changements dans la fréquence et la polarisation produisent des différences mesurables et peuvent être utilisés pour la création d'algorithmes permettant la classification de la glace d'eau douce.

Mots clés: radar à antenne synthétique, glace d'eau douce

Traduit pour le journal par Nésida Loyer.

INTRODUCTION

Monitoring of freshwater ice is important for hydropower generation, ice jams, forecasting, navigation in inland waters, and the construction of winter roads. With the advent in the near future of satellites carrying onboard synthetic aperture radar (SAR), there is an increasing need to evaluate the possibilities and limitations of radar remote sensing in assessing the dynamics of freshwater ice.

During early April 1989 and January 1990, the C/X synthetic aperture radar (SAR) system of the Canada Centre for Remote Sensing (CCRS) was flown over an 80 km stretch of the Burntwood River, Manitoba, Canada, for the detection of freshwater ice features that could lead to a better understanding of the ice regime and to an improved management of river flows regulated for hydropower production. The study was undertaken by MacLaren Plansearch Inc. (now MacPlan), on behalf of Manitoba Hydro and in cooperation with the Canada Centre for Remote Sensing.

The Burntwood River originates northeast of Flin Flon, Manitoba, and discharges into Split Lake, Manitoba. The study area is located at an approximate latitude of 55° north (see Fig. 1). In 1976, the Burntwood River began to receive a mean estimated diversion of 760 m^3/s from the Churchill River system, increasing its pre-diversion mean annual flow by approximately ninefold. This diversion has greatly altered the hydraulic regime of the Burntwood River and subsequent downstream water bodies. Of particular interest are post-diversion ice dynamics and their management, given the reversal of seasonal flows and levels through the altered system for hydropower generation purposes. There exists a strong need for improved methods of studying post-diversion ice formation, movement, and accumulation dynamics to facilitate optimized river management and improved transportation safety.

Specifically, the potential of SAR for identifying open water areas, ice jams, hanging ice dams, frazil ice, and other features of interest to Manitoba Hydro was investigated using C- and X-band data collected by the C/X SAR. The section of the Burntwood River under analysis is characterized by yearly occurrences of major ice accumulation and frazil ice formation, especially along a stretch — approximately 20 km long from First Rapids through a sharp bend, called "the Elbow" — in the river course.

BACKGROUND

Radar signals interact with lake and river ice in a number of ways. Different image target signatures are the result of changes in the physical properties of the ice itself, due to differences in the surface geometry and the roughness characteristics of the ice relative to the parameters of the imaging radar (frequency, polarization, and incidence angle). The dielectric

[1]Canada Centre for Remote Sensing, 1547 Merivale Road, 4th Floor, Ottawa, Ontario, Canada K1A 0Y7
[2]MacPlan, 600 – 5 Donald Street, Winnipeg, Manitoba, Canada R3L 2T4

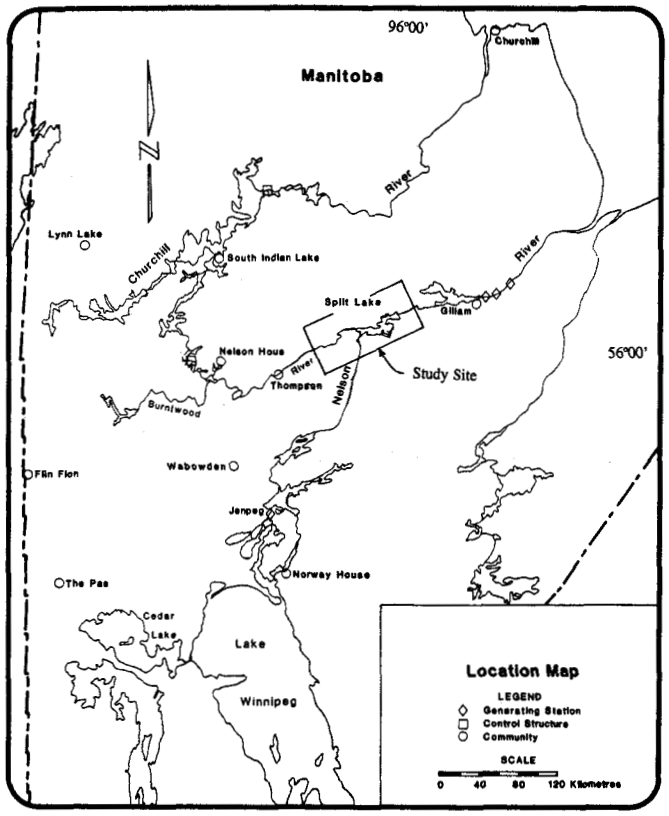

FIG. 1. Study area.

properties of ice are an important factor underlying these mechanisms.

The dielectric constants of lake and river ice typically have low values, in part because these materials are generally chemically "pure," i.e., they do not contain high concentrations of ionic impurities, which strongly interact with the incident microwave energy. Vickers (1975) has studied the microwave properties of ice from the Great Lakes over a frequency range of 1-18 GHz using coaxial and waveguide techniques. He observed that the real part of the dielectric constant of ice was virtually frequency and temperature independent, with values ranging from 3.0 to 3.2, depending on the amount of air inclusions present in the ice samples. Cooper *et al.* (1976) found that for lake ice, the dielectric constant varied from 3.17 for clear ice, to 3.08 for milky ice, to 2.99 for clear ice with large (>0.6 cm) air bubbles. Measurements were taken at a temperature of –10°C over a frequency range of 1-18 GHz.

As a result of the low dielectric values of lake and river ice, much of the incidence microwave energy will penetrate the surface layer, where it is subject to volume scattering. Vickers (1975) noted that pure ice is virtually without absorption loss, and the losses that were measured in ice samples that contained a significant volume of inclusions were clearly due to scattering rather than due to dielectric absorption. Measured losses by Vickers ranged from 2 to 8 dB/m. He also observed a consistent increase in loss as the ice temperature increased, but the effect was small as compared to that caused by air inclusions. Onstott and Moore (1983), using a helicopter-borne microwave active spectrometer operating at C-band (5.3 GHz) frequency, measured the scattering cross-section of first-year sea ice, multi-year sea ice, and freshwater ice for various incidence angle (10-70°) and polarization combinations. The scatter from multi-year sea ice — which is analogous to freshwater ice in terms of ionic composition — showed a slow rate of decay with incidence angle, suggesting a stronger contribution of volume scattering resulting from penetration of the microwave energy into the ice.

Further complication of the scattering mechanisms may be expected in the case of lake and river ice. Because of the small thickness (1-2 m) characterizing lake and river ice, as compared to sea ice, the microwave energy can possibly penetrate the entire ice layer. The radar signal is then subject to complex backscatter mechanisms, involving the contribution of volume scattering effects within the ice layer, surface scattering from the upper ice/air interface and the lower ice/water interface, and, in situations where water freezes to the ground beneath, scattering from the ice/ground interface.

Remote sensing studies of lake and river ice have employed a number of different sensors and approaches. Impulse radar systems have been highly successful when used on the ground and in aircraft for quantitative measurement of ice thickness (Campbell and Orange, 1974; Cooper *et al.*, 1976; Dean, 1981). Swift *et al.* (1980) used a C-band stepped frequency microwave radiometer over the Great Lakes and demonstrated the capability of a microwave radiometer to detect pressure ridges, rubble piles, ship leads, and average changes in the base thickness of ice. Gatto (1988) analyzed a series of Landsat images of the Allegheny and Monongahela rivers taken from 1972 to 1985 to describe the evolution of the river ice cover and the recurrence of distinct ice features. Sellmann *et al.* (1975a) used 1973 Landsat imagery (band 7) to analyze sequential changes in ice cover on oriented lakes to infer lake depth on a regional scale on the Coastal Plain of Alaska. Wiesnet (1979) employed NOAA visible imagery to study ice conditions on Lake Erie.

Comparatively fewer studies have dealt with the utilization of imaging radars (synthetic and real aperture radars) to investigate lake and, in particular, river ice conditions.

Side looking airborne radar imagery has been obtained over northern Alaska to observe oriented lakes, and the images were studied by several investigators (Sellmann *et al.*, 1975b; Elachi *et al.*, 1976; Weeks *et al.*, 1977, 1978, 1981). These investigators noticed that two different categories of lakes rendered distinctly different radar responses: a) lakes that were found to be frozen to the bottom gave low returns, and b) lakes that were not frozen to the bottom gave higher returns when observed using both X- and L-band radars. Stronger radar reflections occur at interfaces with a greater contrast in dielectric constants. The dielectric discontinuity between freshwater ice and water is 3.2/80, which is much higher than that between ice and frozen sediment (3.2/8). Thus lake ice that has water below will give higher radar reflections than lake ice frozen to the lake bed. However, this alone cannot explain the observed effects, as at the non-perpendicular angles at which the radar beam encounters the comparatively flat ice-water interfaces much of the energy would be reflected away from the sensor, even with a highly reflective ice/water boundary present. The numerous elongated air bubbles usually present in ice act primarily as forward scatterers, and in situations where the lake is not frozen to the bottom, stronger radar reflections at the ice/water interface will result in an increased volume scattering and correspondingly stronger radar returns.

Bryan and Larson (1975) classified freshwater lake ice into several distinct categories using airborne X- and L-band radar data in Whitefish Bay and the Straits of Mackinak, Michigan. The ice types identified ranged from smooth black ice (low returns) to very rough ice (high returns). Their analysis of ice in Whitefish Bay indicated that the combination ice/water and ice/air interfaces were the major contributors to the radar backscatter as seen on the imagery. Larrowe *et al.* (1971) identified pressure ridges, wave-induced ripples in loose pack ice, water on ice, and the ice/water interface of X-band SAR imagery of Whitefish Bay. Parashar *et al.* (1978) investigated SAR X- and L-band imagery (HH and HV) of Lake Melville and Grand Lake, Labrador. Their major findings were that: a) there was a reversal in tonal contrast between X- and L-band imagery for some lake ice features; b) a contrasting band around the borders of Valley Bay — a part of Lake Melville — was caused by complete freezing of the lake to its bottom around the borders; c) there can be sufficient penetration of the ice cover by the radar at X- and L-bands so that the difference in the reflection coefficients at the ice/water interface will be apparent; and d) changes in ice porosity, thickness, and roughness at the ice/water interface were responsible for the variety of radar returns exhibited.

Melloh and Gatto (1990) analyzed a series of airborne SAR images along the Tanana River, near Fairbanks, Alaska, and on nearby lakes, under both wet and dry snow conditions. The imagery were acquired with the Jet Propulsion Laboratory's SAR in quad-polarized (HH, VV, HV, and VH) C-, L-, and P-bands. Results confirmed that SAR could be used to identify ice jams, open water, lake ice, and river ice with varying degrees of roughness. In addition, it was concluded from a preliminary investigation that L-band was better overall at distinguishing ice conditions.

SAR DATA COLLECTION

The study area is illustrated in Figure 1 (see also Figs. 2, 3). The communities of Split Lake and York Landing are located within the study area, as is the Manitoba Hydro generating station at Kelsey, on the Nelson River. The Nelson, Burntwood, and Odei rivers flow through the study area and into Split Lake. Additional larger lakes within the study area include Assean and Orr lakes. The terrain is generally typical of northern shield areas, with marshy, low-lying areas, areas of exposed bedrock, and vegetated uplands. River shorelines are usually characterized by rocky, steep slopes.

The SAR data was collected by the airborne C/X-SAR system owned and operated by the Canada Centre for Remote Sensing (CCRS). This system is in service onboard a Convair-580 aircraft. The system operates at C- and X-band (5.3 and 3.2 GHz) frequencies, is capable of transmitting on either horizontal or vertical polarizations and receiving both polarizations simultaneously, and can also operate at various viewing geometries: the narrow swath mode, covering incidence angle from 45 to 76° at 6000 m flight altitude, with a swath width of 18 km; the nadir mode, which covers incidence angles from 0

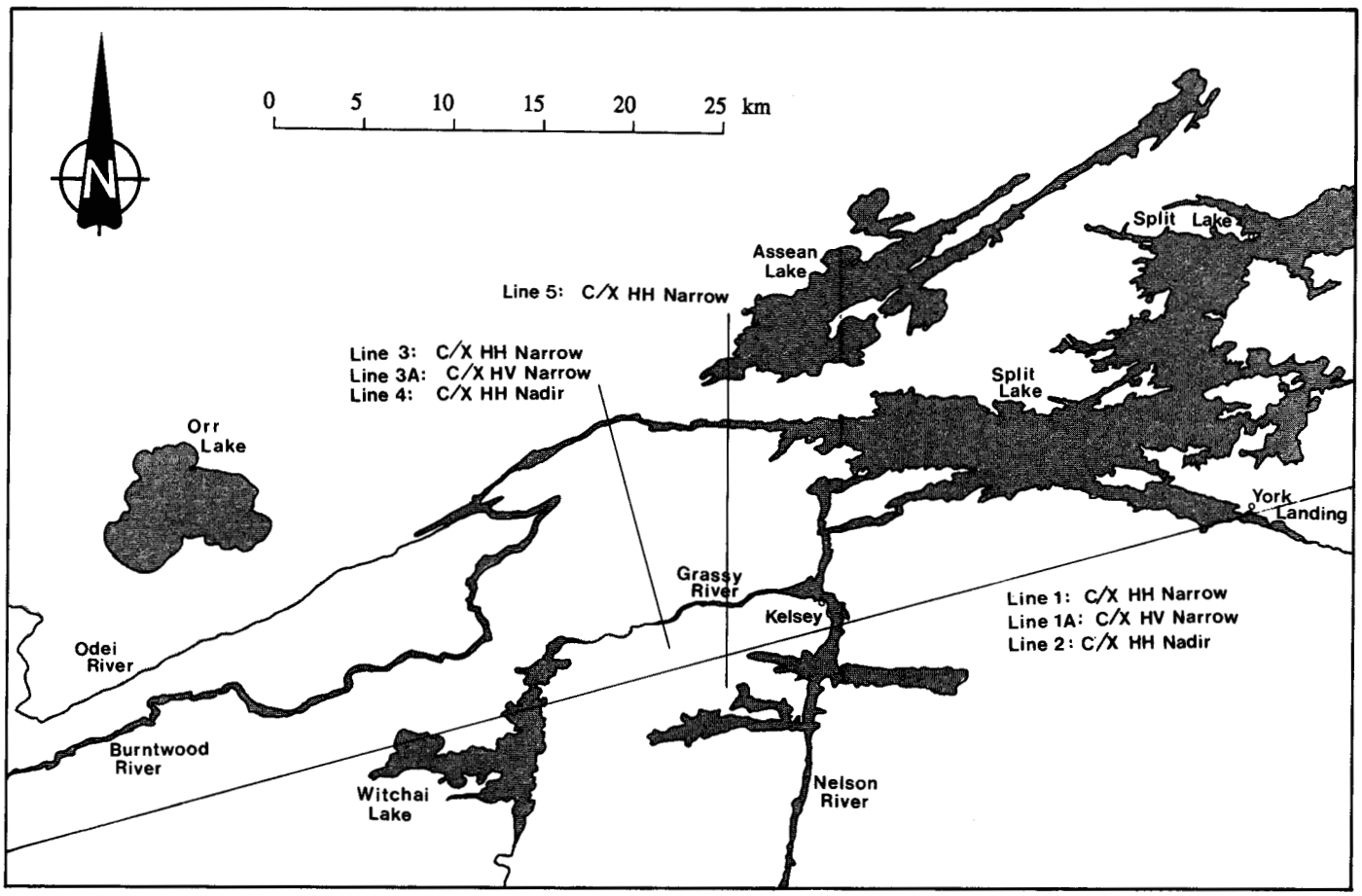

FIG. 2. C/X airborne SAR flight lines.

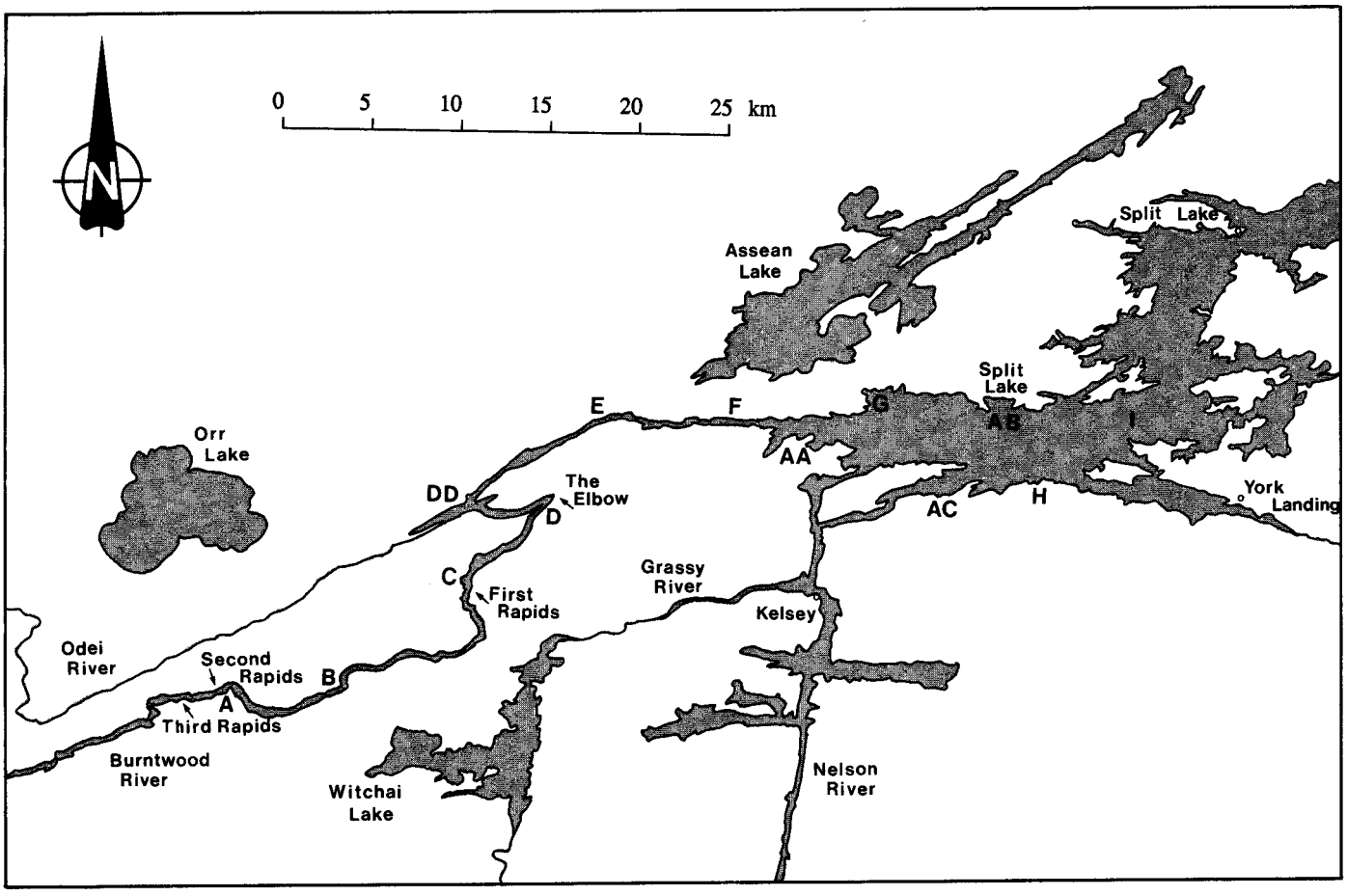

FIG. 3. Location of ground calibration sites.

to 74°, with a corresponding swath width of 22 km; and the wide swath mode, with incidence angles ranging from 45 to 85° and a corresponding swath width of 63 km. Outputs from the C/X SAR system include a dry-silver paper image ("quick look"), an image high-density digital tape (8-bit HDDT) generated by a real-time processor (RTP) onboard the aircraft and delivered in real-time, a videotape produced in real-time, and a signal HDDT (16-bit), which requires further processing on the ground. Detailed description of the system is found in Livingstone *et al.* (1988).

A total of six flight passes were flown on 5 April 1989 and seven flight passes on 4 January 1990 along the Burntwood River and Split Lake, covering a total image length of about 325 and 380 km respectively. Three flight lines were flown along the direction of flow of the Burntwood River into Split Lake, covering a distance of approximately 80 km from the westernmost site, called Third Rapids, to the east end of Split Lake. Three flight lines were also flown perpendicular to the first three lines that imaged a section of the Burntwood River — "The Elbow" — characterized by yearly occurrences of major ice accumulation, jams, and frazil ice formation. In addition, during the January 1990 mission, one flight line was flown approximately perpendicular to the Burntwood River at the entrance to Split Lake, covering the west section of the lake. The location of the flight lines are shown in Figure 2. Table 1 describes the SAR system parameters (viewing geometry, polarization, frequencies, look direction) used in this study. A judicious choice of system parameters has allowed various sections of the Burntwood River, Split Lake, and surrounding shallow lakes to be imaged under a number of different combinations of viewing geometries, polarizations, look directions, and frequencies, facilitating investigation of the effects of these parameters on the resulting imagery and ice features.

TABLE 1. SAR system parameters used in the April 1989 and January 1990 missions

Line	Frequency	Imaging geometry	Polarization	Look direction
1	C/X	Narrow (45-76°)	HV	North
2	C/X	Nadir (0-74°)	HH	North
1	C/X	Narrow (45-76°)	HH	North
3	C/X	Narrow (45-76°)	HH	West
3	C/X	Narrow (45-76°)	HV	West
4	C/X	Nadir (0-74°)	HH	West
1	C/X	Narrow (45-76°)	HH	North
1A	C/X	Narrow (45-76°)	HV	North
2	C/X	Nadir (0-74°)	HH	North
3	C/X	Narrow (45-76°)	HH	West
3A	C/X	Narrow (45-76°)	HV	West
4	C/X	Nadir (0-74°)	HH	West
5*	C/X	Narrow (45-76°)	HH	East

*Line 5 was flown only on the January 1990 mission.

It should be mentioned here that, in order to carry out a truly quantitative analysis in which the radar imagery would be used to infer, if possible, parameters such as ice thickness, it is essential that the imagery be calibrated. Calibration of the imagery allows quantitative comparison of the brightness of targets common to two or more images. To that end, four active radar calibrators (ARC) were deployed at two locations near the Elbow during the April 1989 mission. The purpose of deploying ARCs is to produce on a radar image a series of point targets of known radar cross-section. These point targets are then used to adjust or correct the pixel brightness values of the image for direct comparison of radar images. Unfortunately, cold temperatures on the day of the SAR data acquisition resulted in a malfunctioning of all four ARCs. No ARCs were deployed during the January 1990 mission. However, CCRS is currently working on the development of a methodology to calibrate SAR images based only on internal, i.e., system's, parameters. A preliminary version of the resulting calibration software was recently completed and will be used in the quantitative (i.e., digital) analysis of the Burntwood River images.

Ground data collection was undertaken on the Burntwood River and Split Lake 3-6 April 1989. General ice conditions were established during a reconnaissance helicopter flight on 3 April 1989, at which time the number of pre-selected ground calibration sites were reduced from 13 to 9 as a result of open water leads and unsafe ice conditions. Ground calibration site locations are indicated on Figure 3. Ground data collection was completed over the subsequent three-day period, centred around the SAR flight overpass on 5 April 1989.

At each ground calibration site, measurements and observations were taken that would enable interpretation of the resultant radar imagery and facilitate the characterization of each of the snow, ice, and water layers at each site along the Burntwood River and Split Lake. Snow measurements collected included thickness, a description of each visible layer, crystal size in each layer, and an assessment of snow moisture content. Ice cores (100 mm diameter) were also extracted at each calibration site and were assessed in the field in order to describe visible layering, air content, sediment content, and various inclusion patterns or anomalies. Ice thickness was measured from an auger hole (200 mm diameter) through the ice. Water measurements taken from the auger hole included water depth, temperature, conductivity, salinity, and flow rate. In addition, depth of slush and frazil ice flows under the static ice layer were measured and characterized.

A similar campaign was conducted during the January 1990 mission. And since the quick look imagery could this time be delivered immediately following the flight, other sites showing "anomalous" radar returns were also visited and additional snow and ice measurements were taken. Those site locations are also indicated on Figure 3. A relevant field data summary has been included (Table 2).

RESULTS AND DISCUSSION

Preliminary examination of the April 1989 and January 1990 imagery revealed subtle variations in the radar signatures of the Burntwood River and Split Lake with changes in polarization, incidence angle, and look direction. These variations in tone and texture are best handled through a careful digital analysis of the data set, which is currently under way. The present section focuses exclusively on the interpretation of the C-band HH data taken at narrow swath mode, partly because Radarsat, as it stands now, will be equipped with a C-HH SAR system, and also because the airborne narrow swath imagery does not suffer from severe image distortions in the near range.

Burntwood River

Figure 4 shows the April 1989 airborne C-HH SAR image of the Burntwood River (line 1, see Table 1) covering the "Elbow" area. The image encompasses a surface area of approximately 300 km^2. The data set was acquired at narrow swath mode, with the 45° incidence angle line located at the bottom of the imagery (south) and the 76° incidence angle line located at the top (north). The flow rate in the Burntwood

TABLE 2. Ground calibration site field data summary

Site I.D.	Snow depth (cm)	Ice depth (m)	Ice stratification description	Slush depth (m)	Water depth (m)
April 1989 mission					
A	27.0	1.3	Slush ice/blue ice/ heavy slush	7.5 (to bottom)	none
B	24.0	1.1	Slush ice (layers)/ moderate slush	6.9	4.0
C	40.0	1.1	Slush ice/ juxtaposition ice/heavy slush	10.8 (to bottom)	none
D	22.0	1.3	Layered juxtaposition and slush ice/ moderate slush	6.0	2.7
E	36.0	0.9	Slush ice/blue ice (layers)/moderate slush	2.0	11.9
F	31.0	0.6	Slush ice/blue ice (layers)/moderate slush	3.2	0.03
G	16.5	0.9	Black ice	none	1.1
H	18.0	0.9	Black ice	none	4.1
I	18.0	1.0	Black ice	none	12.9
January 1990 mission					
C	18.0	1.1	Juxtaposition ice /slush ice/ heavy slush	10.0 (est.)	6.0 (est.)
D	17.0-27.0	0.5-0.8	Layered juxtaposition ice/ slush ice/heavy slush	11.5	6.0
DD	16.0	0.4	White and slush ice	none	2.0
E	18.0	0.4-0.8	Juxtaposition ice/ slush ice	none	10.7
F	15.0-25.0	0.4-0.5	White ice/ snow/slush ice	none	3.6
G	22.0	0.6	Black ice	none	1.1
H	10.0	0.8	Black ice	none	2.7
I	12.0	0.7	White ice (6 cm) /black ice	none	12.0
AA	17.0	0.5	Slush ice (10 cm) /black ice	none	2.1
AB	18.0	0.6	Slush ice (30 cm) /black ice	none	14.6
AC	17.0	0.5	Black ice	none	9.9

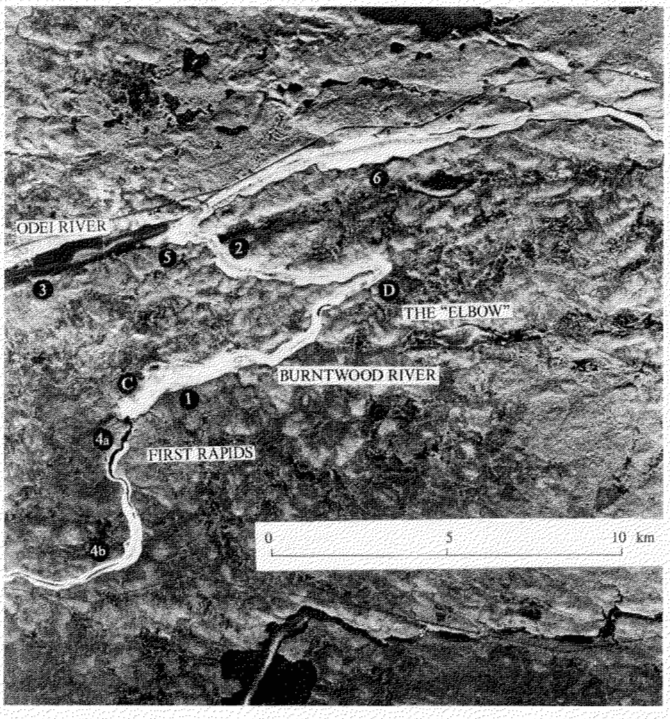

FIG. 4. C-HH narrow swath mode SAR image — "The Elbow" — April 1989.

River is from west to east (left to right on the imagery). During the day of the April SAR mission, the daily flow rate was 790 m^3/s, air temperature was about −15°C, and the snowpack was dry. Under these conditions, it was assumed that the contribution of the snowpack to the total backscatter was small, as dry snow is generally considered to be transparent at C-band frequencies (Rott *et al.*, 1988).

Figure 4 shows that the Burntwood River is generally characterized by high backscatter values (bright returns). The texture of the returns varies from very homogeneous along the riverbanks (see for example location 1 in Fig. 4), to a mottled appearance in the middle of the channel (see location 2 in Fig. 4). In addition, the signature of the Burntwood River contrasts sharply with that of the Odei River, a small tributary discharging at the Elbow (see location 3 in Fig. 4). Flow rates in the Odei River are typically 1-2 orders of magnitude less than the Burntwood River, and flow velocities are also much lower, partly due to backwater effects from the Burntwood. The flow rates in the Odei River were not available for the day of the SAR flight; however flow rates on the preceding 31 December (1988) were measured at 808 m^3/s and 3.5 m^3/s for the Burntwood and the Odei Rivers respectively. It is therefore reasonable to assume that the flows in the Odei River the day of the SAR flight were considerably less than that of the Burntwood. Thus, it appears likely that the brightness of the signatures found on the Burntwood River is related in some complex fashion to the hydraulic regime (flow rates, velocity) of the river.

The ground data set available (see Fig. 3 and Table 2), although limited, nevertheless allowed identification of the most probable mechanisms responsible for the unusually strong returns characterizing the Burntwood River.

Ice cores extracted along the downstream from First Rapids and at the Elbow (sites C and D on Fig. 4) during the April mission revealed an extremely jagged surface, with massive juxtaposition ice over deep slush. The ice cores at the Elbow (site D) showed as many as 8 layers of juxtaposition ice (rafted plates) and white (or slush) ice. Some layers were extremely dirty with clay particles and had air bubbles present. This high stratification of the ice cover is probably the result of the formation and subsequent break-up of a thin ice layer during the initial freeze-up period of the river, causing pile-ups of ice plates and snow. Ashton (1986) notes that "agglomerate ice," which is essentially an agglomeration of individual ice pieces that have refrozen, is frequently found in areas of turbulent flows or rapids in rivers. The ice cores did not provide any definitive clues on the roughness of the ice/water interface, although ice plates were noted at the base of the cover. Ice surface at site B was also rough (see Table 2), with a corresponding coarse texture on the radar imagery (not shown here). On the other hand, site A, which had a smoother surface (See Table 2), displayed a comparatively less mottled texture on the radar imagery (not shown here), although the overall brightness of the radar signature was similar to that at sites B, C, and D. Examination of the ice cores therefore seems to support the hypothesis that volumetric scattering and multiple reflections between the ice/air, and possibly the ice/water, interface and scatterers within the ice matrix are mainly responsible for the high returns and mottled texture found in the Burntwood River. No ice cores were extracted along the Elbow in areas of uniform radar backscatter during the April 1989 mission, and therefore the backscattering mechanisms and river ice characteristics that would explain these radar returns could not be identified with absolute certainty. However, the uniformity of the radar signal strongly suggests that small scatterers (air bubbles, sediments, unfrozen slush, as opposed to juxtaposition ice) would be important contributing elements to the total radar return. Similar tones and textures of the radar return were also observed in other locations along the Burntwood River (see, for example, location 6 in Fig. 4).

Alford and Carmack (1987a,b) have examined the various processes of formation and decay of the ice cover in the Yukon River for two consecutive winters. They observed that during the freeze-up period the formation of the ice cover undergoes a series of steps, starting first with the formation of frazil ice, followed by frazil deposition, lateral growth of shore ice, and formation and gradual closing of a narrow channel by the advance of an ice front. In view of Alford and Carmack's observations of freshwater ice formation in a northern river, and from the SAR signatures and concurrent ground measurements, we propose the following model for the strong radar returns characterizing the Burntwood River: during the freeze-up period, massive amounts of frazil, which agglomerated to form frazil slush and floes, were transported with the flows and adhered to the banks to form shore ice. In areas where the river channel widens (see, for example, location 6 in Fig. 4), the frazil slush may completely cover the reach. Ashton (1986) and Michel and Ramseier (1969) note that it is possible that an entire ice cover could consist of congealed frazil slush. The existence of a uniformly strong radar return seen along the shores of the river is best explained by complex scattering mechanisms occurring in congealed frazil slush. This hypothesis is substantiated by observations of ice core samples extracted near the shore at site F, where a two-layer ice cover constituting a relatively thin (15-20 cm) layer of congealed slush on top of a 50 cm layer of clear ice having a low bubble

content was observed. Closing of the ice cover gradually occurred by the advance of an ice front, made of slush ice and rafted ice plates, in a narrow channel formed along the core velocity. The mottled appearance characterizing very rough surfaces can be observed on the imagery (see, for example, locations 2 and 6 in Fig. 4), and it clearly delineates the river ice run.

If the above assumptions are correct, the strong radar returns observed on the April 1989 imagery would have appeared during or soon after the initial freeze-up period and would have remained over the course of the winter. The January 1990 image of the Burntwood River displays similar backscatter characteristics, thereby reinforcing the hypothesis that the high returns are linked to freeze-up related processes. Figure 5 shows the C-HH narrow swath image of the Elbow, acquired during the January 1990 mission (line 1). Air temperature at the time of the SAR flight was –29°C. Strong, uniform radar returns along the shores and the river ice run (see locations 2 and 6 in Fig. 5 respectively) are again clearly seen on the image.

The hypothesis that the bright returns seen along the Burntwood River originate from refrozen slush is further supported by the radar signatures observed at the Burntwood River – Odei River junction (see location 5 in Figs. 4 and 5). On both SAR missions, a sharp edge between areas of strong and low returns (dark areas) at the confluence is noted. The roughly triangular shape characterizing the area of strong returns indicates that the frazil ice may have "spilled" into the confluence, a consequence of backwater effects from the Burntwood River into the Odei River. An ice core extracted at the confluence (site DD) revealed the presence of a 0.4 m layer of slush ice.

Finally, areas of very low backscatter values were observed on both SAR missions (see locations 4a and 4b in Figs. 4 and 5). Ground observations and oblique aerial photographs confirmed the presence of open water leads at each of these sites. The leads on the January 1990 imagery appear larger than on the April 1989 imagery, which is consistent with the fact that the ice cover during the January 1990 mission was still forming (see Fig. 6). The ice floes appearing on the aerial photography taken west of First Rapids (Fig. 6) are not readily apparent on the corresponding SAR image, because most of the microwave energy reaching the slush-water surface is reflected specularly away from the radar. Although there was visually a good agreement between the width of the open water leads as seen from the radar imagery and from the corresponding aerial photography, a discrepancy was noted at site 4b on the April 1989 data set. There, the lead observed on the SAR imagery appeared much larger than seen on the aerial photograph. It appears that the ice cover immediately next to the lead exhibits characteristics of an almost transparent target at C-band frequency. The existence of this ice cover can best be explained as follows: on 31 March and 3 April the air temperature rose to 8.7 and 4.4°C respectively (see Table 3), resulting in the thinning of the ice cover, the creation of new leads, and the widening of existing open water leads, such as the one in 4b. This was confirmed through helicopter reconnaissance flights on 3 April. As the temperature dropped slightly below the freezing mark on 1, 2, 4, and 5 April (see Table 3), the lead at location 4b began to close again. The newly formed ice was thin and uniform, exhibiting all the characteristics of a low-scattering medium (small amounts of impurities, specular reflection at the ice/water and ice/air interfaces).

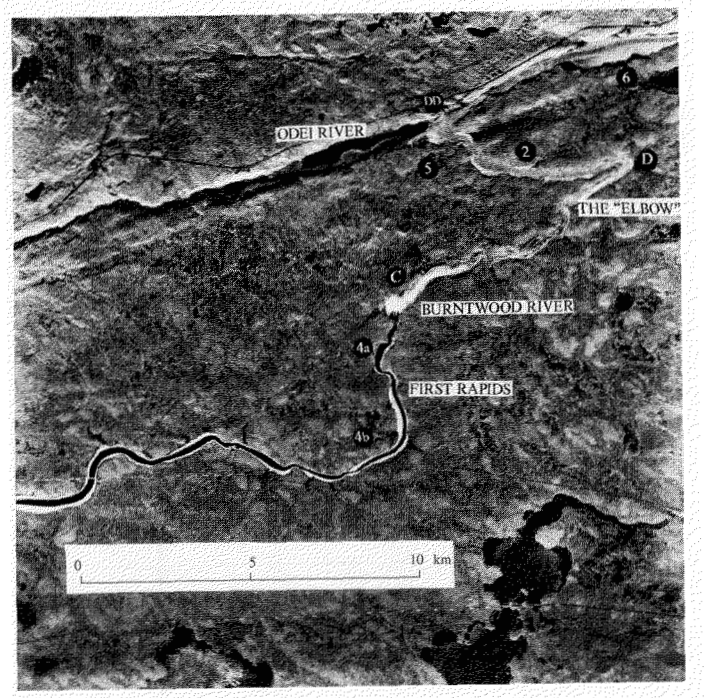

FIG. 5. C-HH narrow swath mode SAR image — "The Elbow" — January 1990.

FIG. 6. Ice cover formation, First Rapids, January 1990.

Split Lake

Figures 7 and 8 show the airborne C-HH SAR imagery (line 1) acquired during the April 1989 mission and covering the west and central sections of Split Lake and sections of the Burntwood and Nelson rivers. The west and central sections of the lake, imaged during the January 1990 mission, are shown

TABLE 3. Ambient air temperature at Thompson, Manitoba, April 1989 mission

Day	Tmin	Tmax	Tmean
25/03/89	-19.3	-9.2	-14.3
26/03/89	-21.1	-14.0	-17.0
27/03/89	-23.9	-13.8	-18.7
28/03/89	-20.8	-12.6	-16.4
29/03/89	-21.2	-6.6	-14.0
30/03/89	-24.7	1.0	-10.3
31/03/89	-6.0	8.7	0.0
01/04/89	-3.0	0.0	-1.8
02/04/89	-9.7	-1.3	-5.0
03/04/89	-10.5	4.4	-2.4
04/04/89	-11.1	-2.7	-6.3
05/04/89	-19.5	-6.8	-12.9

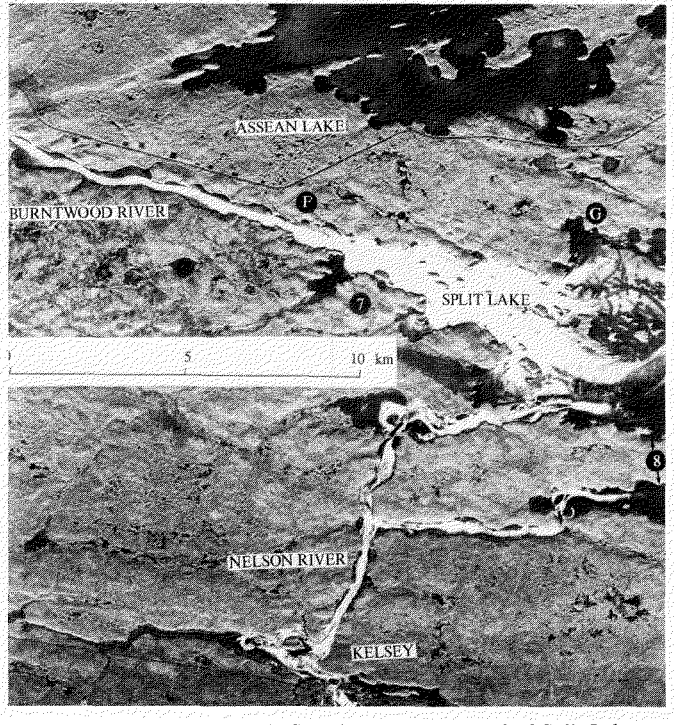

FIG. 7. C-HH narrow swath mode SAR image — west end of Split Lake — April 1989.

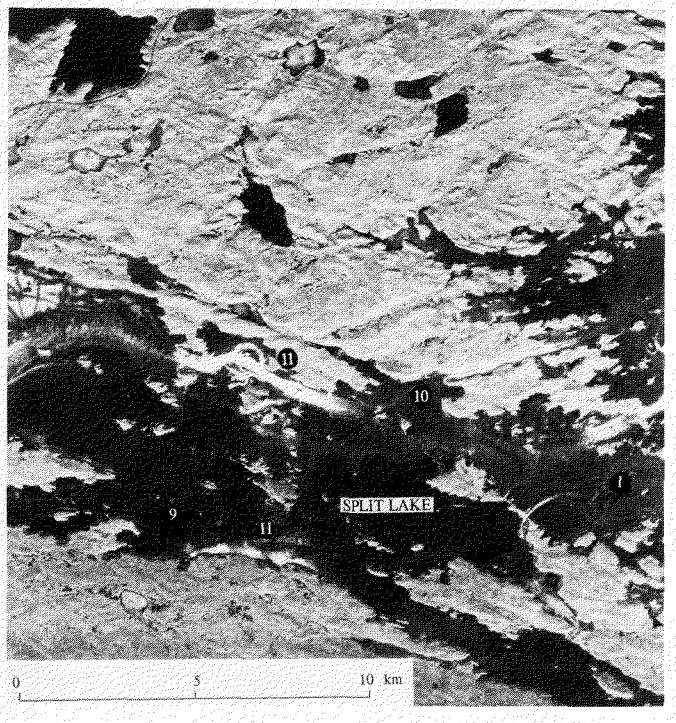

FIG. 8. C-HH narrow swath mode SAR image — central Split Lake — April 1989.

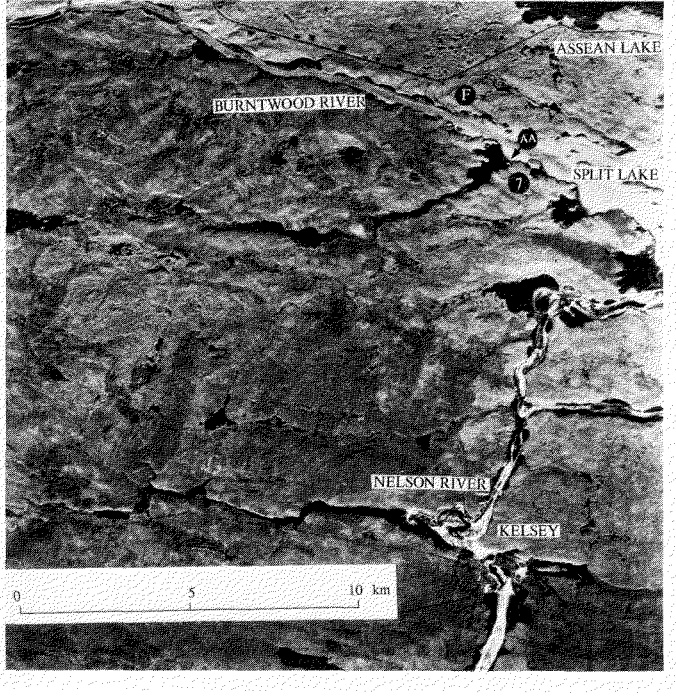

FIG. 9. C-HH narrow swath mode SAR image — west end of Split Lake — January 1990.

in Figures 9 and 10 respectively (line 1).The imagery was acquired at narrow swath mode, and each figure covers an area of approximately 300 km^2.

Lake ice formation, decay, and stratigraphic and crystalline structure differ from those of river ice. Typical lake ice covers have snow ice above lake ice (also called black ice). Ashton (1986) reports that numerous mechanisms are responsible for the formation of snow ice, among which are: 1) snow deposition on a thin ice cover, which depresses the ice cover, allowing lake water to rise through cracks into the overlying snow, and 2) the percolation of rain and melting snow, which refreezes in the lower levels of the snowpack. Typically, lake ice grows downward into the water column by a process called congelation, in which the heat of crystallization is conducted upward through the existing ice column. The ice/water boundary resulting from this process is usually very smooth. Another characteristic of lake ice is the incorporation of small elongated gas bubbles into the ice during the freezing process. Such bubbles begin to appear "whenever the rejection of gas at the ice/water interface is rapid enough to cause the water's gas content to exceed its nucleation level" (Gow and Langston, 1977:13). In addition, slow-growing ice will incorporate larger air bubbles if air is trapped beneath the ice.

Congelation and formation of smooth ice surfaces are responsible for the generally dark radar signatures characterizing lake ice (see, for example, location 9 in Fig. 8), in which the subtle tonal variations of the radar returns (see, for example, location 10 in Fig. 8) are related to the presence of a higher concentration of scatterers (e.g., air bubbles).

In particular, the western portion of the lake, where the Burntwood River discharges its waters (see location 7 in Figs. 7 and 9), and channels in the central and northern section (see location 11 in Figs. 8 and 10) exhibit similarity in tone and texture to those returns found along the Burntwood River (see, for instance, location 6 in Figs. 4 and 5). These observations suggest that similar backscattering mechanisms and ice cover types are involved — i.e., that the strong returns seen in both SAR missions in the west section of Split Lake originate from the formation of frazil slush that congealed during the freeze-up period. Ashton (1986) has reported that congealed frazil slush is found in rivers, but it can also be found in reservoirs and lakes fed by turbulent waters. Ice cores extracted at the lake entrance in January 1990 (see site AA in Fig. 9) confirmed the presence of a two-layer ice cover similar to that found along the Burntwood River. In particular, a large ice block was extracted at site AB (see Fig. 10). It revealed the existence of a congealed slush layer of 0.3 m thickness (Fig. 11). Furthermore, when the ice cover was punctured with a metal bar, water started filling in the hole well before reaching completely through the congealed slush layer, indicating the likely presence of unfrozen slush. Gow and Langston (1977:6) note that "water saturated snow (slush) normally freezes from top down so that it is not unusual to find layers of unfrozen slush sandwiched between lake ice and snow ice." The existence of unfrozen slush in the ice cover, which could result in a rough unfrozen-frozen slush boundary, is another possible contributing factor to the overall brightness of the returns observed at sites AA and AB. The validity of this hypothesis could not be assessed for the Burntwood River due to insufficient ground measurements.

Figures 7 and 9 show that the areas encompassed by refrozen slush are considerable, covering most of the west entrance to Split Lake. The spread and location of the high radar returns strongly suggest that the slush originated from the Burntwood River and was transported into the lake, which is consistent with observations reported by Ashton (1986). If the formation of the frazil slush was a lake-induced process, other large open areas in the lake would normally present conditions favourable to frazil formation (e.g., turbulent flows resulting from wind action), and thus other large areas of bright radar returns would be expected. With the exception of some channels in Split Lake (see, for example, location 11 in Figs. 8 and 10) where the constriction of flows between islands and the shore would funnel the flow of slush ice during freeze-up, the overall signature is that of lake ice, with no evidence of massive frazil ice generation. Although the above observations support the hypothesis that the strong returns observed along these channels are also the result of slush originating from the Burntwood River, this assumption could not be verified due to the lack of ground data and of aerial photographs taken during the lake ice formation period.

An interesting overall pattern is observed in Split Lake: most of the high radar returns are found along the north shore area, although Split Lake is also fed by another important river, the Nelson, with flows exceeding those of the Burntwood. Figures 7 and 9 show a small section of the Nelson River, which discharges its waters in the southwest portion of Split Lake. In particular, the very strong radar signals characterizing the west entrance to Split Lake are almost totally absent from the southwest entrance (see location 8 in Figs. 7 and 9). The Nelson River is regulated by a series of hydraulic structures required for hydroelectric power generation, while the Burntwood River currently does not produce any hydroelectric power. A generating station is located at Kelsey, approximately 10 km to the south and east of Split Lake (see bottom of Figs. 7 and 9). This station acts as a barrier to the incoming frazil slush, therefore, and although frazil will be generated between Kelsey and Split Lake, the quantities produced seem insufficient to completely cover the southern entrance to the lake. Ice cores and ice slabs extracted at the

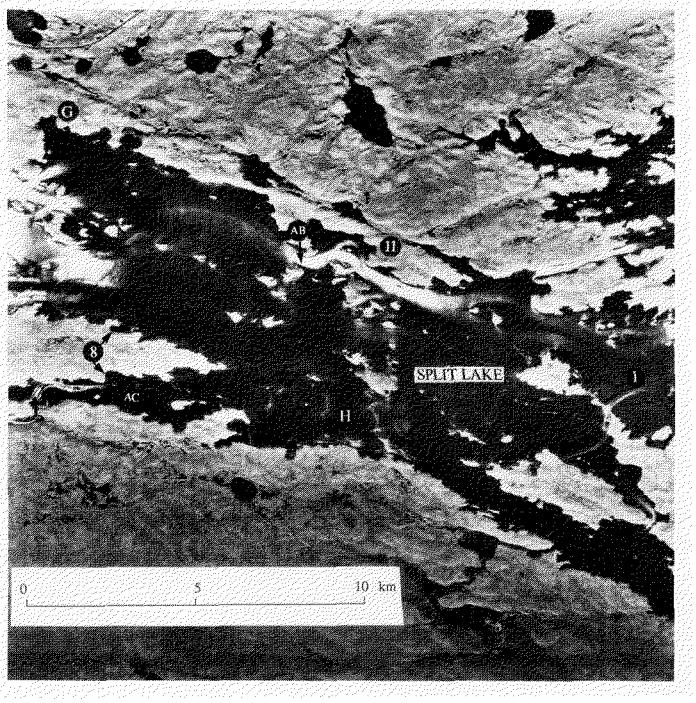

FIG. 10. C-HH narrow swath mode SAR image — central Split Lake — January 1990.

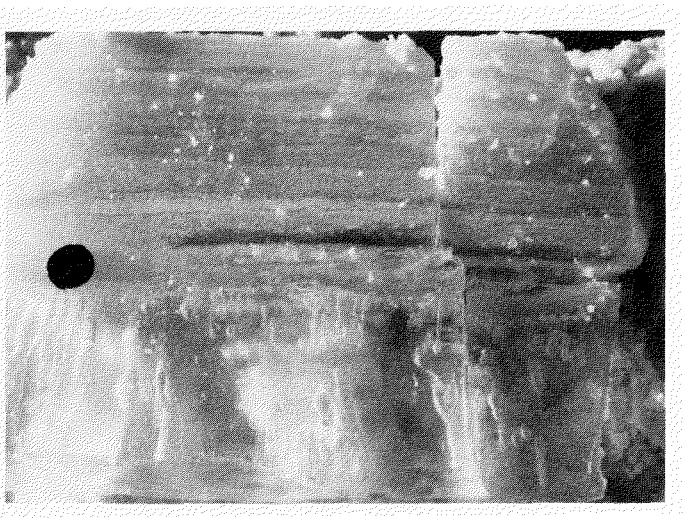

FIG. 11. Ice slab removed at Split Lake, location AB, 5 January 1990.

southern entrance (see site AC in Fig. 10) during the January 1990 mission were all characterized by a single layer of lake ice, with few bubbles, and did not show any presence of refrozen slush.

In addition to the very bright returns observed in Split Lake, the north section of the lake is generally characterized by an overall slightly brighter return than its southern portion (see Figs. 8 and 10). A SPOT image acquired during October 1990 clearly shows sediment patterns with a sharp high/low edge concentration of sediment running east-west (Fig. 12). This demarcation reflects the large differences in sediment concentration in the Burntwood (high sediment content) and the Nelson (low sediment content) rivers and also indicates that the waters coming from these two rivers do not mix together until well into Split Lake. Extrapolation of the case above to the situation where frazil slush is being transported into Split Lake therefore provides one explanation to the generally stronger radar signal in the northern section of the lake (high frazil slush content), as opposed to the low returns found in its southern portion (low frazil slush content). Ice cores extracted in the northern portion of Split Lake (see site I in Figs. 8 and 10) revealed a thin layer of white ice (1-2 cm). This contrasted with the relatively "pure" lake ice found in its southern portion (see site AC in Fig. 9).

ONGOING ANALYSES

The data set generated during the April 1989 and January 1990 SAR missions is voluminous (a total of 33 image computer compatible tapes) and a thorough analysis of the data will take a significant amount of time. Digital analysis of the April 1989 imagery to separate and quantify the effects of the various image geometry, frequency, and polarization combinations through georeferencing and overlay analysis is nearing completion. Preliminary interpretation suggests that frequency and polarization differences (such as between C-HH and X-HH, and C-HV and C-HH) produce measurable differences in radar backscatter for certain types of river and lake ice. Additional digital analysis will focus on the development of a classified SAR image based on the ground calibration site data and reconnaissance flight observations, a multitemporal comparison of the April 1989 and January 1990 data sets, and the integration of the SAR data with simultaneously acquired SPOT data during January 1990. The possibility of acquiring a third data set to investigate specific anomalies noted during analyses of the first two data sets is being considered.

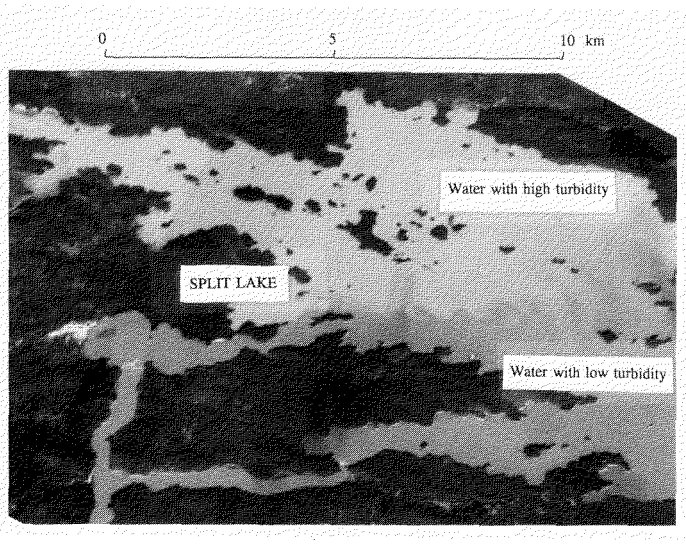

FIG. 12. SPOT image from 25 October 1990 — Burntwood River and Split Lake.

CONCLUSIONS

Multichannel SAR data have been examined for a stretch of the Burntwood River and Split Lake in northern Manitoba. Strong radar returns from the Burntwood River have been explained through a proposed ice freeze-up model in which primary river ice forms from congealed frazil slush, which can reach across the entire river channel, and possibly from the presence of unfrozen slush in the river ice cover. The bright, mottled radar signatures on the Burntwood River close to the Elbow have been accounted for by the presence of extremely stratified ice (layered white slush ice and juxtaposed ice plates that overlie heavy slush), which causes volumetric scattering and multiple reflections from the ice/water and ice/air interfaces and from scatterers within the ice matrix.

The generally dark radar signatures from Split Lake have been accounted for by the typically smooth ice/water interfaces found on the lake, with the observed subtle tonal variations within the lake attributed to the varying presence of scatterers (air bubbles) within the ice matrix. Unexpectedly bright radar responses from the lake have been attributed to the presence of slush ice, originating in the Burntwood River, forming the primary ice cover and/or the constriction of flows between islands and the shore, which funnels the flow of slush ice during freeze-up, and the presence of unfrozen slush in the ice matrix.

REFERENCES

ALFORD, M.E., and CARMACK, E.C. 1987a. Observations on the ice cover and streamflow in the Yukon River near Whitehorse during 1983/1984. IWD Scientific Series No. 152, Paper No. 32. Saskatoon: National Hydrology Research Institute. 63 p.

_____. 1987b. Observations on the ice cover and streamflow in the Yukon River near Whitehorse during 1984/1985. IWD Scientific Series No. 155, Paper No. 34. Saskatoon: National Hydrology Research Institute. 24 p.

ASHTON, G.D. 1986. River and lake ice engineering. Fort Collins, Colorado: Water Resources Publications.

BRYAN, M.L., and LARSON, R.W. 1975. The study of freshwater lake ice using multiplexed imaging radar. Journal of Glaciology 14(72):445-457.

CAMPBELL, K.J., and ORANGE, A.S. 1974. Continuous sea and freshwater ice thickness using an impulse radar system. In: Santeford, H.S., and Smith, J.L., eds. Advanced concepts and techniques in the study of snow and ice resources, U.S. Hydrological Decade. Washington, D.C.: National Academy of Sciences. 432-443.

COOPER, D.W., MUELLER, R.A., and SCHERTLER, R.J. 1976. Remote profiling of lake ice using an S-band short-pulse radar aboard an all-terrain vehicle. Radio Science 11:375-381.

DEAN, A.M., Jr. 1981. Electromagnetic subsurface measurements. Special Report SR 81-23. Hanover, New Hampshire: Cold Regions Research and Engineering Laboratory.

ELACHI, C., BRYAN, M.L., and WEEKS, W.F. 1976. Imaging radar observations of frozen arctic lakes. Remote Sensing of Environment 5:169-175.

GATTO, L.W. 1988. Ice conditions along the Allegheny and Monongahela rivers as observed on Landsat images, 1972-1985. Special Report 88-6. Hanover, New Hampshire: Cold Regions Research and Engineering Laboratory. 106 p.

GOW, A.J., and LANGSTON, D. 1977. Growth history of lake ice in relation to its stratigraphic, crystalline and mechanical structure. Report 77-1.

Hanover, New Hampshire: Cold Regions Research and Engineering Laboratory. 24 p.

LARROWE, B.T., INNES, R.B., RENDLEMAN, R.A., and PORCELLO, R.J. 1971. Lake ice surveillance via airborne radar: Some experimental results. Report MS-7, Vol. 1. Ann Arbor: The University of Michigan.

LIVINGSTONE, C.E., GRAY. A.L., HAWKINS, R.K., and OLSEN, R.B. 1988. CCRS C/X airborne synthetic aperture radar: An R and D tool for the ERS-1 timeframe. IEEE Aerospace and Electronics Systems Magazine 3(10):11-20.

MELLOH, R.A., and GATTO, L.W. 1990. Interpretation of passive and active microwave imagery over snow-covered lakes and rivers near Fairbanks, Alaska. In: Proceedings of the Workshop on Applications of Remote Sensing in Hydrology, Saskatoon, Saskatchewan, 13-14 February. 259-278.

MICHEL, B., and RAMSEIER, R.O. 1969. Classification of river and lake ice based on its genesis, structure and texture. Report 5-15, Université Laval, Faculté des sciences, Département de génie civil, Section mécanique des glaces. 40 p.

ONSTOTT, R.G., and MOORE, R.K. 1983. C-band measurements of radar backscatter from ice. RSL Technical Report 524-Final. Lawrence: Remote Sensing Laboratory Centre for Research, Inc., The University of Kansas. 26 p.

PARASHAR, S.K., ROCHE, C., and WORSFOLD, R.D. 1978. Four channel synthetic aperture radar imagery results of freshwater ice and sea ice in Lake Melville. C-CORE Publication 78-11. St. John's: Memorial University, Centre for Cold Ocean Resources Engineering. 16 p.

ROTT, H., MATZLER, C., STROBL, D., BRUZZI, S., and LENHART, K.G. 1988. Study on SAR land applications for snow and glacier monitoring. ESA Contract No. 6618/85/F/FL (SC). Innsbruck: Universitat Innsbruck. 186 p.

SELLMANN, P.V., BROWN, J., LEWELLEN, R.I, McKIM, H., and MERRY, C. 1975a. The classification and geomorphic implications of thaw lakes on the Arctic Coastal Plain, Alaska. Report RR 344. Hanover, New Hampshire: Cold Regions Research and Engineering Laboratory.

SELLMANN, P.V., WEEKS, W.F., and CAMPBELL, W.J. 1975b. Use of side-looking airborne radar to determine lake depth on the Alaska North Slope. Special Report 230. Hanover, New Hampshire: Cold Regions Research and Engineering Laboratory. 10 p.

SWIFT, C., HARRINGTON, R.F., and THORNTON, F. 1980. Airborne microwave radiometer remote sensing of lake ice. In: Proceedings of the IEEE Electronics and Aerospace Systems Convention, 29-30 September and 1 October 1980. 369-373.

VICKERS, R.S. 1975. Microwave properties of ice from the Great Lakes. SRI Project 3571. Menlo Park: Stanford Research Institute. 25 p.

WEEKS, W.F., SELLMANN, P., and CAMPBELL, W.J. 1977. Interesting features of radar imagery of ice covered North Slope lakes. Journal of Glaciology 18(78):129-136.

WEEKS, W.F., FOUNTAIN, A.G., BRYAN, M.L., and ELACHI, C. 1978. Differences in radar return from ice-covered North Slope lakes. Journal of Geophysical Research 83(C8):4069-4073.

WEEKS, W.F., GOW, A.J., and SCHERTLER, R.J. 1981. Ground-truth observations of ice-covered North Slope lakes imaged by radar. Report 81-19. Hanover, New Hampshire: Cold Regions Research and Engineering Laboratory. 17 p.

WIESNET, D.R. 1979. Satellite studies of freshwater ice movement on Lake Erie. Journal of Glaciology (24):415-426.